

國立交通大學

電子工程學系 電子研究所

碩士論文

時空編碼與多路徑分集特論

On Space-Time Codes with Multipath Diversity

研究生：吳承祐

指導教授：桑梓賢 教授

中華民國九十五年八月

時空編碼與多路徑分集特論

On Space-Time Codes with Multipath Diversity

研究生：吳承祐

Student : Cheng-yu Wu

指導教授：桑梓賢

Advisor : Tzu-Hsien Sang

國立交通大學

電子工程學系 電子研究所



Submitted to Department of Electronics Engineering & Institute of Electronics

College of Electrical Engineering and Computer Science

National Chiao Tung University

in partial Fulfillment of the Requirements

for the Degree of

Master

in

Electronics Engineering

August 2006

Hsinchu, Taiwan, Republic of China

中華民國九十五年八月

時空編碼與多路徑分集特論

研究生： 吳承祐

指導教授： 桑梓賢 博士

國立交通大學

電子工程學系 電子研究所碩士班

摘要

時空編碼是一種可以從多重天線系統中得到分集增益的編碼技術。它可以分成兩大類:時空區塊編碼和時空籬柵編碼。在[1]和[2]分別對這兩種編碼方式在平緩衰減通道中的情形有詳細的討論。在本論文中，我們結合時空編碼和 MLSE 演算法來處理因為頻率選擇性通道所造成的交互位元干擾，並且得到額外的多路徑分及增益來增進系統的效能。另外，我們提出了一種時空籬柵編碼的編碼方式，這種編碼可以和通道結合，在接收端做聯合解碼來增進效能。另一方面，將會把提出的演算法和其他相關的演算法做比較。最後，會使用模擬結果來驗證這個演算法的分集階數和效能。

On Space-Time Codes with Multipath Diversity

研究生：吳承祐

student : *Cheng-yu Wu*

指導教授：桑梓賢

Advisors : *Tzu-Hsien Sang*

Department of Electronics Engineering & Institute of Electronics
National Chiao Tung University

ABSTRACT

Space-Time coding is a coding technique to achieve the diversity gain of multiple antennas system. Two popular space-time codes, space-time block code (STBC) and space-time trellis code (STTC), are investigated in [1] and [2] for flat fading channels without intersymbol interference. In this thesis, we extend space-time coding to frequency selective channels. We combine space-time coding with MLSE (Maximum Likelihood Sequence Estimator) algorithms to handle the intersymbol interference and exploit the multipath diversity gain of frequency selective channels. Furthermore we propose a new space-time trellis coding process that combines the coding with the channel effect, and achieve diversity gain by joint decoding at the receiver. On the other hand, we also compare the proposed algorithm with some related algorithm. Finally, simulation results will be presented to verify the diversity order and the performance of the proposed coding scheme.

誌謝

兩年的研究所生活一下就過去了。然而在這短短的兩年，卻學到了很多東西，也有很多收穫。首先這都要謝謝我的指導教授桑梓賢老師，這兩年之中老師對我的研究給予了相當多的建議與指導，讓我可以順利完成畢業論文。除此之外，老師也常常與我們分享他對許多事情的觀點與看法，讓我增長了許多專業領域外的知識。在此還是要再次的謝謝老師。

另外，我也要感謝欣德學長在這兩年之中對我的幫忙。在與他的討論當中我解決了許多研究上遇到的難題，並且學到很多經驗。當然，也要謝謝實驗室其他的學長以及同學們，很高興能認識你們，跟你們一起合作。由於有各位的幫忙，讓我過了兩年充實的研究生生活。

最後，感謝我的家人和朋友在這兩年對我的幫忙和支持，謝謝！



Contents

中文摘要.....	I
ABSTRACT.....	II
誌謝.....	III
CONTENT.....	IV
LIST OF TABLES.....	IV
LIST OF FIGURES.....	V
Chapter 1	1
Introduction	1
1.1 Diversity Order.....	2
1.2 Alamouti Scheme	3
1.3 Time-Reversal Space-Time Block Code.....	5
1.4 Delay Diversity Scheme	9
1.5 Alamouti Scheme with MLSE.....	11
1.6 Summary	14
Chapter 2	17
2.1 Space-Time Trellis Code.....	17
2.2 STTC with MLSE	18
2.2.1 The separated Scheme of STTC with MLSE.....	19
2.2.2 The combined Scheme of STTC with MLSE	20
2.2.3 Simulation	25
2.3 Modulated Code	29
2.4 Space-Time Turbo Equalization.....	35
Conclusion.....	38
Reference.....	39

LIST OF TABLES

Table 1.1 Code rate, complexity and diversity level of delay code	10
Table 1.2 Code rate, complexity and diversity level of three schemes.....	14
Table 1.3 Application and condition of schemes discussed in the chapter	15

LIST OF FIGURES

Figure 1.1 Bit error probability as a function for different T_x	3
Figure 1.2 Alamouti scheme for two transmitters and one receiver	4
Figure 1.3 Transmit scheme of TR-STBC	5
Figure 1.4 Transmit patterns of TR-STBC.....	6
Figure 1.5 Receive scheme of TR-STBC.....	6
Figure 1.6 Bit error rate of TR-STBC with different channel path.....	9
Figure 1.7 Standard delay diversity scheme	10
Figure 1.8 Trellis diagram of Alamouti with MLSE.....	12
Figure 1.9 Bit error rates of Alamouti with MLSE on different path power	13
Figure 1.10 Simulation of Alamouti with MLSE on different channellength.....	14
Figure 2.1 Encoder of STTC.....	17
Figure 2.2 The separated scheme	19
Figure 2.3 The combined scheme	20
Figure 2.4 Trellis structure for code 1.3.....	23
Figure 2.5 Bit error rates of separated scheme and combined scheme.....	26
Figure 2.6 Bit error rates of code 1.1 , 1.2 and 1.3	26
Figure 2.7 Bit error rates of code 2.1 and 2.2	27
Figure 2.8 Bit error rates of combined scheme	28
Figure 2.9 Bit error rates of the different schemes on 2-path channel.....	28
Figure 2.10 Bit error rates of the different schemes on 3-path channel.....	29
Figure 2.11 Transmit scheme of STMC	30
Figure 2.12 STMC ZF-DFE.....	31
Figure 2.13 Simulations of STMC ZF-DFE on channel A and B.....	34
Figure 2.14 Bit error rates of STMC ZF-DFE on Rayleigh fading channel.....	35
Figure 2.15 The structures of transmitter and turbo equalizer.....	36
Figure 2.16 Bit error rates of turbo equalizer.....	37

Chapter 1

Introduction

As wireless communication grows rapidly in the recent years, it is required to provide higher data rates and more reliable services. Use of multiple antennas at receivers and transmitters is an emerging technology to meet this demand without extra power or bandwidth, because multiple antennas systems obtain the spatial diversity and enormous capacity. These studies are presented in [3].

Space-time code is a coding processing for multiple antenna systems to obtain the spatial diversity and temporal diversity. Such codes include, for example, space-time block code (STBC) [5], Alamouti scheme [1], and space-time trellis code (STTC) [2].

However, most studies of space-time codes, such as Alamouti scheme and STTC, assume that there is no intersymbol interference (ISI). If the channel is frequency selective and the transmitted symbols suffer from ISI, Alamouti scheme and STTC will no longer work. In order to handle ISI effects, we suggest a scheme which combines space-time code with MLSE (maximum likelihood sequence estimate) algorithm. MLSE is an optimal estimate which can not only handle ISI but exploit the benefits from multipath channels. Therefore multipath will not cause the distortion but provide the multipath diversity gain. This conception is applied in other systems. For example, RAKE receiver of CDMA system collects paths of channel to improve performance. In OFDM system, FFT algorithm sums all the paths to preserve information of the channel.

Therefore, the scheme that combines space-time coding and MLSE obtains the spatial diversity provided by multiple antennas and the temporal diversity provided by multipath channels. Schemes deployed similar concepts include delay diversity scheme [9],

time-reversal space-time block code (TR-STBC) [5] and modulated code [13]. In this thesis, we focus on the diversity order that each scheme could achieve.

The remaining of this thesis is organized as follows: in chapter 1, we introduce Alamouti scheme, delay diversity scheme and TR-STBC. Then we propose a scheme which combines Alamouti scheme with MLSE and compare the difference among these schemes. In chapter 2, we propose another scheme which combines STTC with MLSE, and compare this scheme with a similar method scheme, called space-time modulated code (STMC) [13].

1.1 Diversity Order

In the thesis we focus on the diversity order that each system can achieve. The maximum diversity order that a system can achieve, called “full diversity order”, is the product of the number of transmit antennas, receive antennas and paths on the channel. In this thesis, we usually use the system with two transmit antennas and one receiver antenna on the channel with L path. Therefore full diversity order is usually $2L$ in this thesis.

We will analysis the diversity order that some space-time systems can achieve. In this thesis we choose a reference system: a system with T_x transmit antennas and one receive antenna. The channel of this reference system is a Rayleigh i.i.d. fading channel with a single path. The average error probability can be explicitly expressed as [18]

$$P_e = \left[\frac{1}{2} \left(1 - \sqrt{\frac{SNR}{1+SNR}} \right) \right]^{T_x} \sum_{k=0}^{T_x-1} \binom{T_x-1+k}{k} \left[\frac{1}{2} \left(1 - \sqrt{\frac{SNR}{1+SNR}} \right) \right]^{T_x} \quad (1.1)$$

where $SNR = \frac{E_b}{T_x N_0}$, E_b is the transmitted bit energy and N_0 is the average noise power. The total transmitted power is the same for each simulation. According to (1.1), the average error probability as a function for different numbers of transmit antennas T_x is illustrated in figure 1.1.

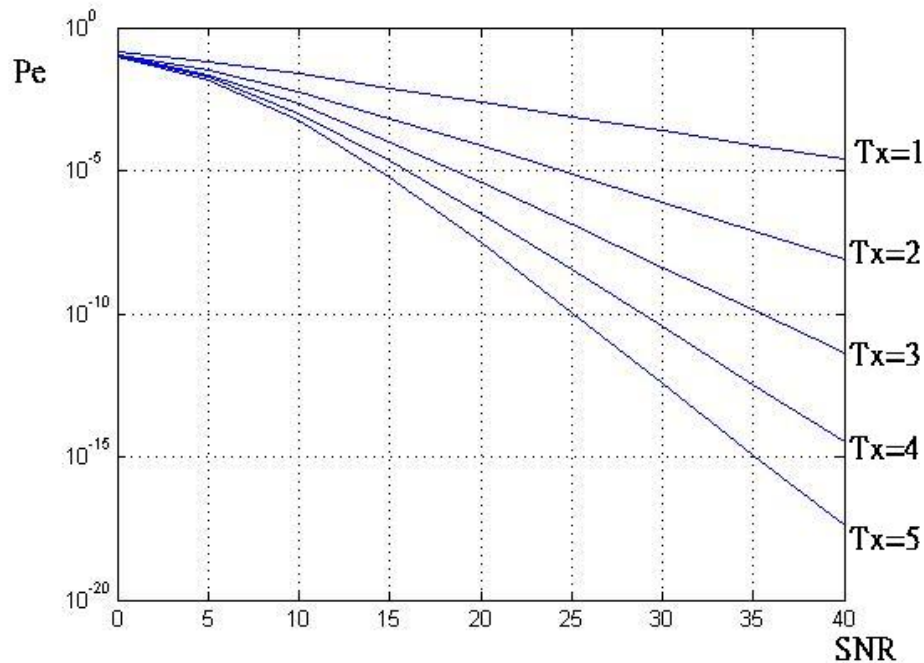


Figure 1.1 Bit error probability as a function for different T_x

In the thesis, we define the diversity order as negative value of the slope of the curve in figure 1.1. If the diversity order that a system can achieve is T_x , it will mean the slope of the error probability curve of this system is equal to the system with T_x transmit antennas and one receive antenna on the Rayleigh fading channel with a single path.

1.2 Alamouti Scheme [1]

In 1998, Alamouti proposed a new coding scheme, called Alamouti scheme, for systems with two transmit antennas on slow fading channels. Alamouti scheme is the first space-time block code to provide full spatial diversity. Figure 1.2 shows the transmit scheme of Alamouti scheme for two transmitters and one receiver.

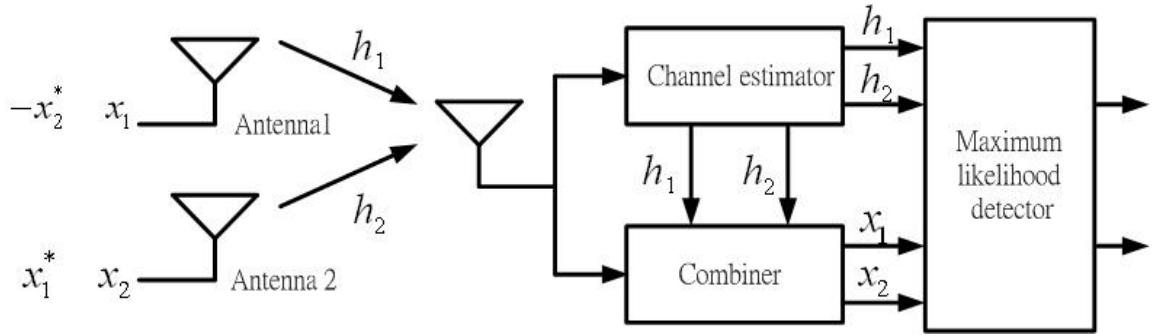


Figure 1.2 Alamouti scheme for two transmitters and one receiver

At a given symbol time t , the signal transmitted from antenna one is denoted by x_1 and from antenna two by x_2 . During the next symbol period symbol $(-x_2^*)$ is transmitted from antenna one, and symbol x_1^* is transmitted from antenna two where $*$ is the complex conjugate operation.

The basic assumption of Alamouti scheme is that the channel is constant over two consecutive symbol periods. The channel between transmit antenna one and receive antenna during t to $t+T$ can be denoted by h_1 and the channel between transmit antenna two and receive antenna during t to $t+T$ by h_2 . Thus the received signals can be expressed as

$$\begin{aligned}
 r_1 &= h_1 x_1 + h_2 x_2 + n_1 \\
 r_2 &= -h_1 x_2^* + h_2 x_1^* + n_2
 \end{aligned}
 \tag{1.2}$$

where r_1 and r_2 are the received signals at time t and $t+T$ and n_1 and n_2 are white Gaussian noise. Then we get the transmit symbols by combining two received signals as follows expression:

$$\begin{aligned}
 \tilde{x}_1 &= h_1^* r_1 + h_2 r_2^* \\
 \tilde{x}_2 &= h_2^* r_1 - h_1 r_2^*
 \end{aligned}
 \tag{1.3}$$

Substituting (1.2) into (1.3) we get:

$$\begin{aligned}\tilde{x}_1 &= (|h_1|^2 + |h_2|^2)x_1 + h_1^*n_1 + h_2n_2^* \\ \tilde{x}_2 &= (|h_1|^2 + |h_2|^2)x_2 - h_1n_2^* + h_2^*n_1\end{aligned}\quad (1.4)$$

These combined signals are then sent to the maximum likelihood detector to decide \mathbf{x}_0 and \mathbf{x}_1 in PSK constellation.

Performance of Alamouti scheme is shown in [1]. Because the structure of Alamouti code is full rank and orthogonal, Alamouti scheme achieves full spatial diversity and is easy to decode on the slow fading channel.

1.3 Time-Reversal Space-Time Block Code

The Alamouti scheme assumes that the channel is flat fading. This will not be the case if the channel experiences a delay spread. Thus, a special STBC called time-reversal space-time block code (TR-STBC) is proposed in [5] [6] [7]. It is an extension of Alamouti scheme to ISI channel. The transmit scheme and the transmit symbol patterns are shown in figure 1.3 and Figure 1.4.

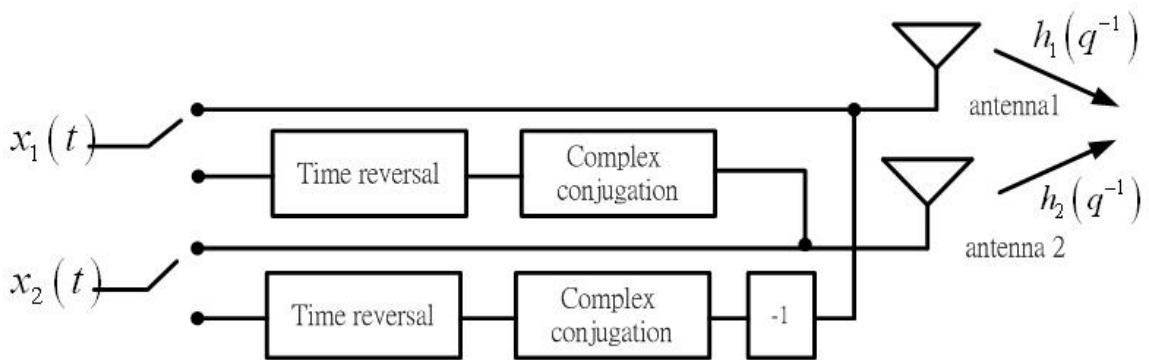


Figure 1.3 Transmit scheme of TR-STBC [5]

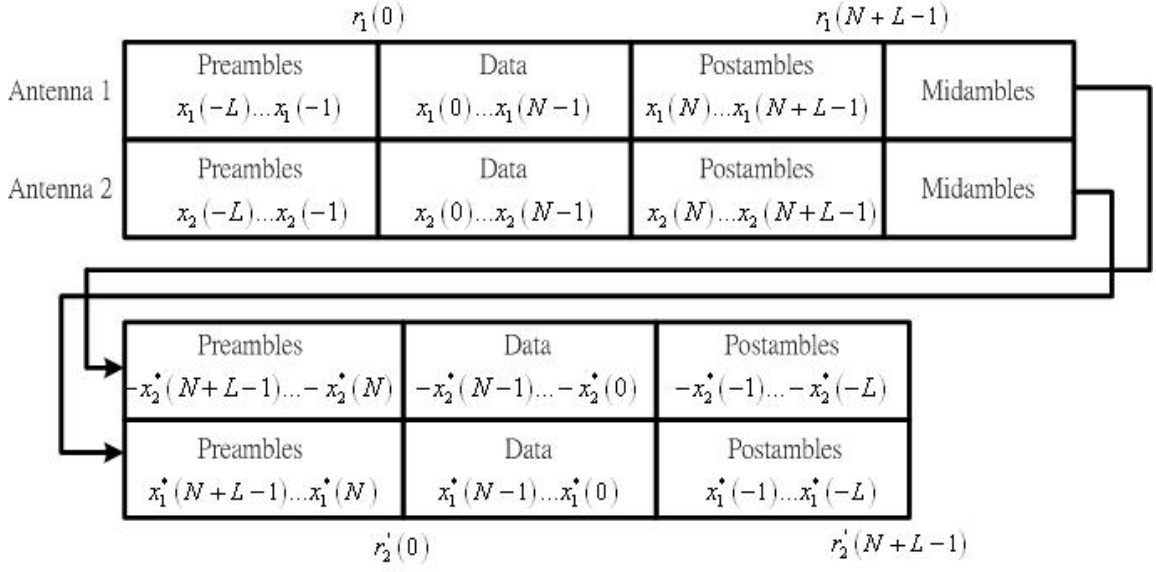


Figure 1.4 Transmit patterns of TR-STBC [6]

Figure 1.5 shows the receive scheme of TR-STBC.

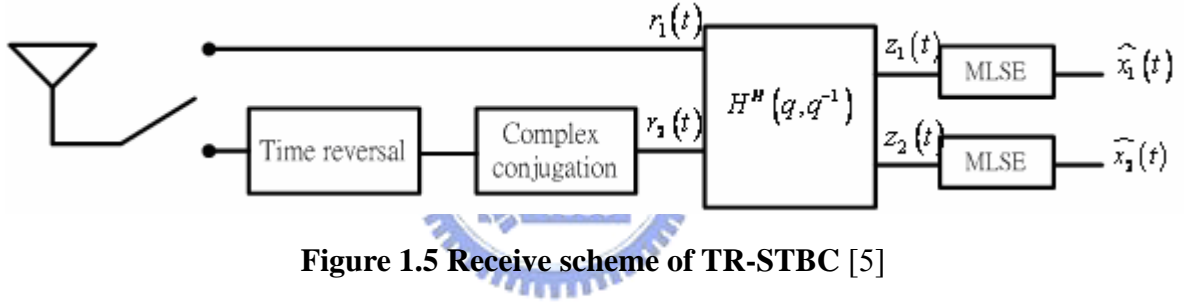


Figure 1.5 Receive scheme of TR-STBC [5]

A discrete time filter will be represented as a polynomial in the unit delay operator, q^{-1} , as follow

$$\begin{aligned}
 v(t) &= a(q^{-1})u(t) = (a_0 + a_1q^{-1} + \dots + a_nq^{-n})u(t) \\
 &= a_0u(t) + a_1u(t-1) + \dots + a_nu(t-n)
 \end{aligned} \tag{1.5}$$

where n is the order of the polynomial.

The complex conjugate of $a(q^{-1})$ is defined as

$$\left(a(q^{-1})\right)^* \triangleq a^*(q) = a_0^* + a_1^*q + \dots + a_n^*q^n \tag{1.6}$$

According to (1.5) and (1.6), for a system with two transmit antennas and one receive antenna, if we transmit symbols denoted by $x_1(t)$ and $x_2(t)$ from antenna one and two, the received signals at every “even” and “odd” symbol time will be

$$\begin{aligned}
r_1(t) &= h_1(q^{-1})x_1(t) + h_2(q^{-1})x_2(t) + n_1(t) \\
r_2'(t) &= h_2(q^{-1})x_1^*(t) - h_1(q^{-1})x_2^*(t) + n_2'(t)
\end{aligned} \tag{1.7}$$

where $h_1(q^{-1})$ and $h_2(q^{-1})$ are the channels for the antenna one and antenna two and $n_1(t)$ and $n_2'(t)$ are the noise at the even and odd symbol times respectively.

We assume that the channel is constant over two consecutive package periods in this scheme, similar to the assumption in Alamouti scheme.

$r_2(t)$ is the complex conjugate of $r_2'(t)$, expressed as

$$r_2(t) = (r_2'(t))^* = h_2^*(q^{-1})x_1(t) - h_1^*(q^{-1})x_2(t) + n_2(t) \tag{1.8}$$

If we introduce the vectors

$$\underline{r}(t) = \begin{bmatrix} r_1(t) \\ r_2(t) \end{bmatrix}, \quad \underline{x}(t) = \begin{bmatrix} x_1(t) \\ x_2(t) \end{bmatrix}, \quad \underline{n}(t) = \begin{bmatrix} n_1(t) \\ n_2(t) \end{bmatrix}$$

and the matrix

$$\underline{\underline{H}}(q, q^{-1}) = \begin{bmatrix} h_1(q^{-1}) & h_2(q^{-1}) \\ h_2^*(q^{-1}) & -h_1^*(q^{-1}) \end{bmatrix}$$

We can express receive signal vector as

$$\underline{r}(t) = \underline{\underline{H}}(q, q^{-1})\underline{x}(t) + \underline{n}(t) \tag{1.9}$$

then we multiply $\underline{r}(t)$ with $\underline{\underline{H}}^H(q, q^{-1})$ just like the decoding process of Alamouti

scheme, we get

$$\begin{aligned}
\underline{z}(t) &= \underline{\underline{H}}^H(q, q^{-1})\underline{r}(t) = \underline{\underline{H}}^H(q, q^{-1})\underline{\underline{H}}(q, q^{-1})\underline{x}(t) + \underline{\underline{H}}^H(q, q^{-1})\underline{n}(t) \\
&= (h_1^*(q)h_1(q^{-1}) + h_2^*(q)h_2(q^{-1}))\underline{x}(t) + \underline{v}(t)
\end{aligned} \tag{1.10}$$

where

$$\underline{v}(t) = \begin{bmatrix} v_1(t) \\ v_2(t) \end{bmatrix} = \underline{\underline{H}}^H(q, q^{-1})\underline{n}(t)$$

Using the components of $\underline{z}(t) = [z_1(t) \ z_2(t)]^T$, we can express (1.10) as

$$\begin{aligned} z_1(t) &= (h_1^*(q)h_1(q^{-1}) + h_2^*(q)h_2(q^{-1}))x_1(t) + v_1(t) \\ z_2(t) &= (h_1^*(q)h_1(q^{-1}) + h_2^*(q)h_2(q^{-1}))x_2(t) + v_2(t) \end{aligned} \quad (1.11)$$

We use MLSE algorithm to decide $\mathbf{x}_1(t)$ and $\mathbf{x}_2(t)$. The branch metric is

$$\begin{aligned} \mu(t) &= \mu(t-1) + \text{Re} \left\{ x_1^*(t) \left(2z_1(t) - \gamma_0 x_1(t) - 2 \sum_{m=1}^n \gamma_m x_1(t-m) \right) \right\} \\ \mu(t) &= \mu(t-1) + \text{Re} \left\{ x_2^*(t) \left(2z_2(t) - \gamma_0 x_2(t) - 2 \sum_{m=1}^n \gamma_m x_2(t-m) \right) \right\} \end{aligned} \quad (1.12)$$

In (1.12), γ_k is defined as follow

$$\gamma(q, q^{-1}) = h_1^*(q)h_1(q^{-1}) + h_2^*(q)h_2(q^{-1}) = \gamma_n^* q^n + \dots + \gamma_0 + \dots + \gamma_n q^{-n} \quad (1.13)$$

The simulation results of TR-STBC system with two transmit antennas and one receive antenna are shown in Figure 1.6. Assuming L is the number of paths on the channel and power of each path is equal, we find that TR-STBC can achieve full temporal and spatial diversity: $2L$. Although TR-STBC can handle ISI and achieve full diversity on the multipath channel, it is not suitable for the channel which changes fast according to the assumption in (1.7).

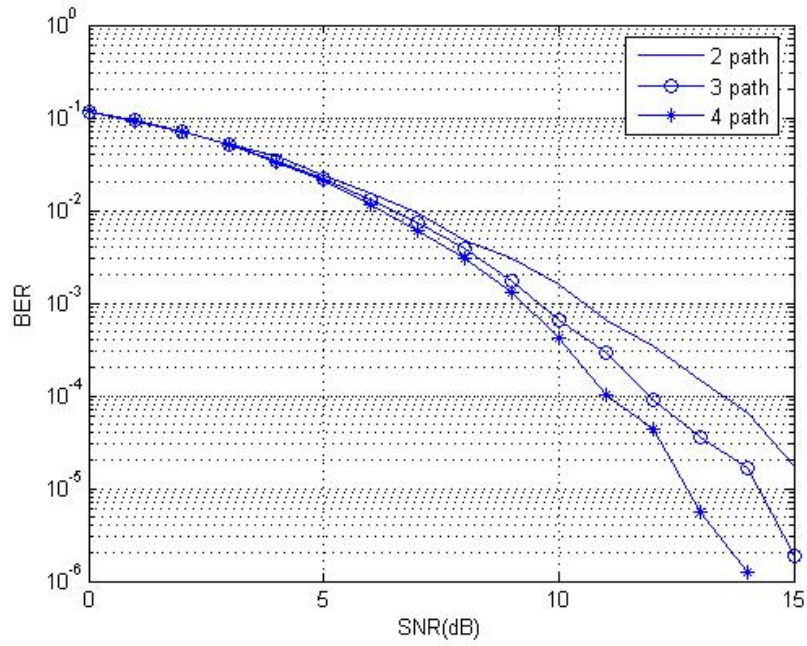


Figure 1.6 Bit error rate of TR-STBC with different channel path

1.4 Delay Diversity Scheme



The delay diversity scheme was proposed in [8] and a similar scheme was suggested in [9] [10]. One of the delay diversity schemes, called standard delay diversity (SDD) scheme is illustrated in Figure 1.7. MLSE algorithm is used to detect the transmitted symbols. In this chapter, we assume T_x and R_x are the number of the transmit antenna and receive antenna respectively, and L is the number of paths on the channel and power of each path is equal. Performance evaluation in [9] and [11] shows that this scheme achieves $T_x \times R_x + 1$ order diversity. Although the SDD scheme guarantees to extract full spatial diversity ($T_x \times R_x$), it can not achieve full diversity ($T_x \times R_x \times L$).

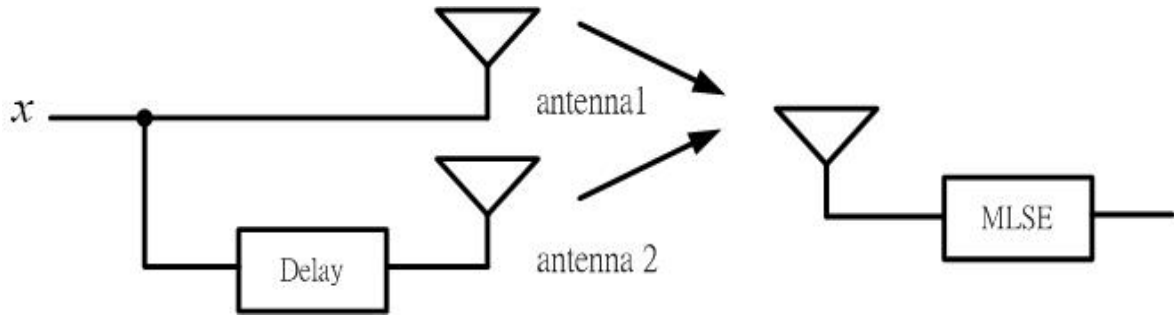


Figure 1.7 Standard delay diversity scheme

To achieve full diversity, an extension of the delay diversity scheme, called generalized delay diversity (GDD) scheme, was proposed in [9] [10]. For a channel of length L , the transmitted symbols of GDD scheme on antenna two is delayed by L symbols. Performance presented in [11] shows that the structure of GDD codeword can achieve full spatial and temporal diversity. However, this structure implies that the longer length of the channel, the more register is used, and the complexity increases exponentially. For a delay code with d delay and BPSK modulation is used, the code rate, complexity and diversity level are listed in table 1.1.

Assuming the channel is ideal and fast enough, delay diversity scheme, unlike Alamouti scheme and TR-STBC, is suitable for fast fading channel.

Code rate	Complexity	Diversity level
$\frac{N}{N+d}$	2^{L+d-1}	$L \leq d: T_x L$ (full diversity) $L > d: d+L$

L : channel length d : delay N : number of symbols in a transmitted package

Table 1.1 Code rate, complexity and diversity level of delay code

1.5 Alamouti Scheme with MLSE

In the section we combines Alamouti scheme with MLSE to exploit the temporal and spatial diversity. We will introduce this scheme and compare it with the others in the next section.

Consider Alamouti scheme discussed in section 1.2, if there are N input symbols, denoted by x_1, x_2, \dots, x_N , the transmitted symbols after encoded will be

$$\begin{bmatrix} \underline{X}_1 \\ \underline{X}_2 \end{bmatrix} = \begin{bmatrix} x_1 & -x_2^* & \dots & x_{i-2} & -x_{i-2}^* & x_i & -x_{i+1}^* & \dots & x_{N-1} & -x_N^* \\ x_2 & x_1^* & \dots & x_{i-1} & x_{i-1}^* & x_{i+1} & x_i^* & \dots & x_N & x_{N-1}^* \end{bmatrix} \quad (1.14)$$

The impulse responses of the frequency selective channel for the antenna one and antenna two denoted by \underline{h}_1 and \underline{h}_2 are

$$\underline{h}_1 = [h_{11}, h_{12}, \dots, h_{1L}], \quad \underline{h}_2 = [h_{21}, h_{22}, \dots, h_{2L}] \quad (1.15)$$

where h_{jk} is the zero-mean complex Gaussian random variable and L is the length of channel. In this section we assume the length of each channel is identical.

The received signal is the convolution of the input symbols and the channel impulse response, which can be expressed as

$$r = \underline{X}_1 \otimes \underline{h}_1 + \underline{X}_2 \otimes \underline{h}_2 + n \quad (1.16)$$

where \otimes denotes the convolution and n is the white noise. Substituting (1.14) and (1.15) into (1.16) we get

$$r(i) = \sum_{k=0}^{\lfloor \frac{L-1}{2} \rfloor} h_{1,2k+1} s_{i-2k} - \sum_{k=0}^{\lfloor \frac{L}{2} \rfloor} h_{1,2k} s_{i-2k+1}^* + \sum_{k=0}^{\lfloor \frac{L-1}{2} \rfloor} h_{2,2k+1} s_{i-2k+1} + \sum_{k=0}^{\lfloor \frac{L}{2} \rfloor} h_{2,2k} s_{i-2k}^* + n(i) \quad (1.17)$$

$$r(i+1) = - \sum_{k=0}^{\lfloor \frac{L-1}{2} \rfloor} h_{1,2k+1} s_{i-2k+1}^* + \sum_{k=0}^{\lfloor \frac{L}{2} \rfloor} h_{1,2k} s_{i-2k+2} + \sum_{k=0}^{\lfloor \frac{L-1}{2} \rfloor} h_{2,2k+1} s_{i-2k}^* + \sum_{k=0}^{\lfloor \frac{L}{2} \rfloor} h_{2,2k} s_{i-2k+3} + n(i+1) \quad (1.18)$$

According to (1.17) and (1.18), we can find that the received signal at i -th symbol time is interfered by last $2^{\lfloor L/2 \rfloor \times 2}$ symbols. Thus if we use B-PSK modulation, the computation complexity of the proposed scheme will be $2^{\lfloor L/2 \rfloor \times 2}$.

Because x_i and x_{i+1} are transmitted at time i and $i+1$, we have to use the received signals at time i and $i+1$ when we will decide x_i and x_{i+1} . The maximum likelihood detection is given by

$$\arg \min_{s_i, s_{i+1}} \sum_{i=1}^N \left\{ \|z(i) - r(i)\|^2 + \|z(i+1) - r(i+1)\|^2 \right\} \quad (1.19)$$

where $z(i)$ and $z(i+1)$ are defined as

$$z(i) = \sum_{k=0}^{\lfloor \frac{L-1}{2} \rfloor} h_{1,2k+1} s_{i-2k} - \sum_{k=0}^{\lfloor \frac{L}{2} \rfloor} h_{1,2k} s_{i-2k+1}^* + \sum_{k=0}^{\lfloor \frac{L-1}{2} \rfloor} h_{2,2k+1} s_{i-2k+1} + \sum_{k=0}^{\lfloor \frac{L}{2} \rfloor} h_{2,2k} s_{i-2k}^* \quad (1.20)$$

$$z(i+1) = - \sum_{k=0}^{\lfloor \frac{L-1}{2} \rfloor} h_{1,2k+1} s_{i-2k+1}^* + \sum_{k=0}^{\lfloor \frac{L}{2} \rfloor} h_{1,2k} s_{i-2k+2} + \sum_{k=0}^{\lfloor \frac{L-1}{2} \rfloor} h_{2,2k+1} s_{i-2k}^* + \sum_{k=0}^{\lfloor \frac{L}{2} \rfloor} h_{2,2k} s_{i-2k+3}^* \quad (1.21)$$

Assuming BPSK modulation is used and channel length is 2, the trellis diagram of the proposed scheme is illustrated in Figure 1.8.

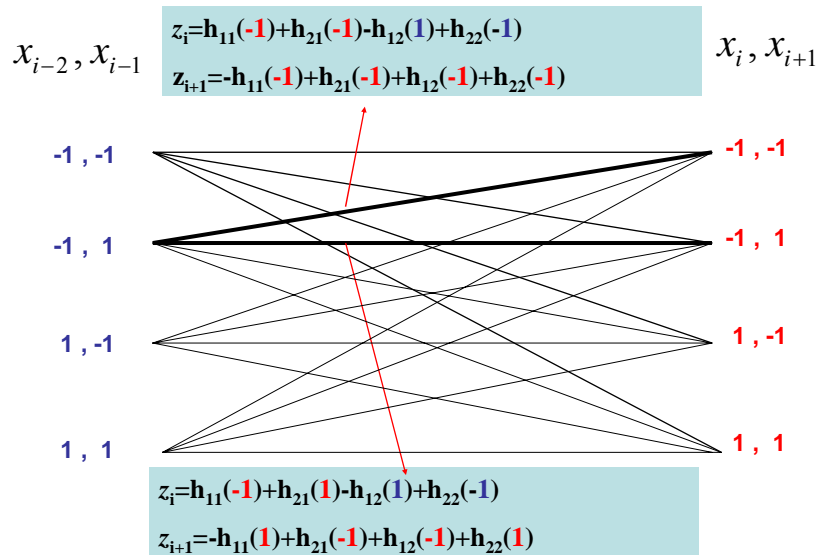


Figure 1.8 Trellis diagram of Alamouti with MLSE

Figure 1.9 shows the simulation results of this scheme for different path power distribution. In this simulation, we assume there are two transmit antennas and one receive antenna in the system. In general, longer channel length and more average power distribution of paths cause more serious ISI. But it also means higher diversity order that the channel can provide. If we use optimal receiver such as MLSE, the performance of the system on the high diversity order channel will be better.

Figure 1.10 shows the simulation results of this scheme for different channel length. For the system with two transmit antennas and one receive antenna, The diversity that the scheme can achieve is $L + 2$, where L is the channel length and the power of each path is the same. We find the diversity order is the sum of L and the number of transmit antennas (denoted by T_x), not the product of L and T_x . Therefore this scheme can not achieve full diversity.

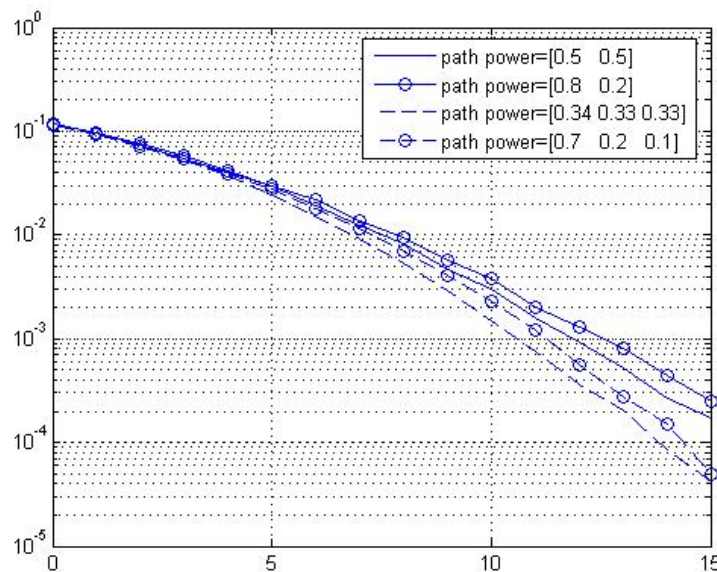


Figure 1.9 Bit error rates of Alamouti with MLSE on different path power

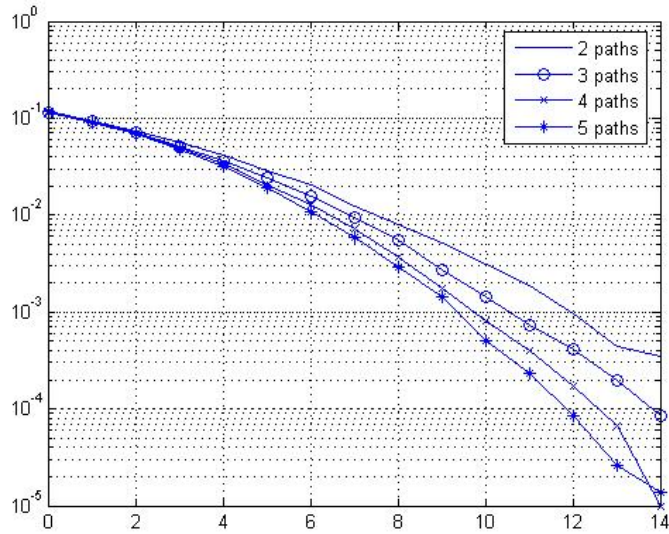


Figure 1.10 Simulation of Alamouti with MLSE on different channel length

1.6 Summary

In the section, we summarize the results from previous sections and compare the difference among TR-STBC, delay diversity scheme and the proposed scheme. The complexity, diversity level and code rate of these scheme are presented in table 1.2. The channel condition for each scheme discussed in the chapter is listed in table 1.3. In this section, we assume there are two transmit antennas and one receiver antenna, i.e. $T_x=2$, $R_x=1$, and BPSK modulation is used.

	TR-STBC	Delay diversity scheme	Alamouti scheme with MLSE
Code rate	$\frac{N}{N + 2(L-1) + L_M}$	$\frac{N}{N + d}$	1
Complexity	2^L	2^{L+d-1}	$2^{\lfloor L/2 \rfloor \times 2}$

Diversity level	$2L$ (full diversity)	$L \leq d$: $2L$ (full diversity) $L > d$: $d+L$	$d+L$
------------------------	-----------------------	---	-------

N : number of symbols in a transmitted package

L : channel length d : delay

L_M : length of midamble

Table 1.2 Code rate, complexity and diversity level of three schemes


	Condition	Applied channel
Alamouti scheme	channel is constant over two symbol times no ISI	Slow flat fading
TR-STBC	channel is constant over two package times	Slow fading frequency selective
Delay diversity scheme		fast fading frequency selective
Proposed scheme		fast fading frequency selective

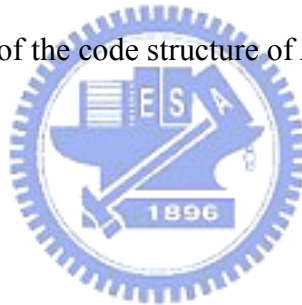
Table 1.3 Application and condition of schemes discussed in the chapter

From table 1.2, we find that TR-STBC achieves full diversity no matter how long the length of channel. But the code rate of TR-STBC is the lowest of these three schemes. If the number of symbols in a package, denoted by N , is large, the code rate will approach one and the comparison of the code rate is not meaningful. But remember that we assume the channel is constant over two consecutive package periods. If the channel changes fast, the number of symbols in a package will be small, and the code rate of TR-STBC will decrease. Because of these reasons, TR-STBC may not adapt to the fast fading channel.

Then consider delay diversity scheme. This scheme permits the change of the channel

during a package periods. Thus, the code rate of delay diversity scheme will approach one if N is large enough. The encoder structure of delay diversity scheme is simple, and if the number of the delayed symbols is equal to the channel path (GDD), this scheme will achieve full diversity. But when the channel length is long, GDD scheme will increase the number of delayed symbols to achieve full diversity, and the complexity will increase rapidly. Although delay diversity scheme can be applied on the fast fading frequency selective channel and achieve full diversity, we have to balance the complexity with diversity level.

Alamouti scheme with MLSE achieves highest code rate and lowest complexity among these three schemes, and it can be applied on the. fast fading frequency selective channel just as delay diversity scheme. The disadvantage is that the proposed scheme can not achieve full diversity because of the code structure of Alamouti scheme.



Chapter 2

2.1 Space-Time Trellis Code

Space-Time trellis code (STTC), which was first introduced in [2], can provide substantial coding gain and full spatial diversity on the flat fading channel. The encoder structure is shown in figure 2.1:

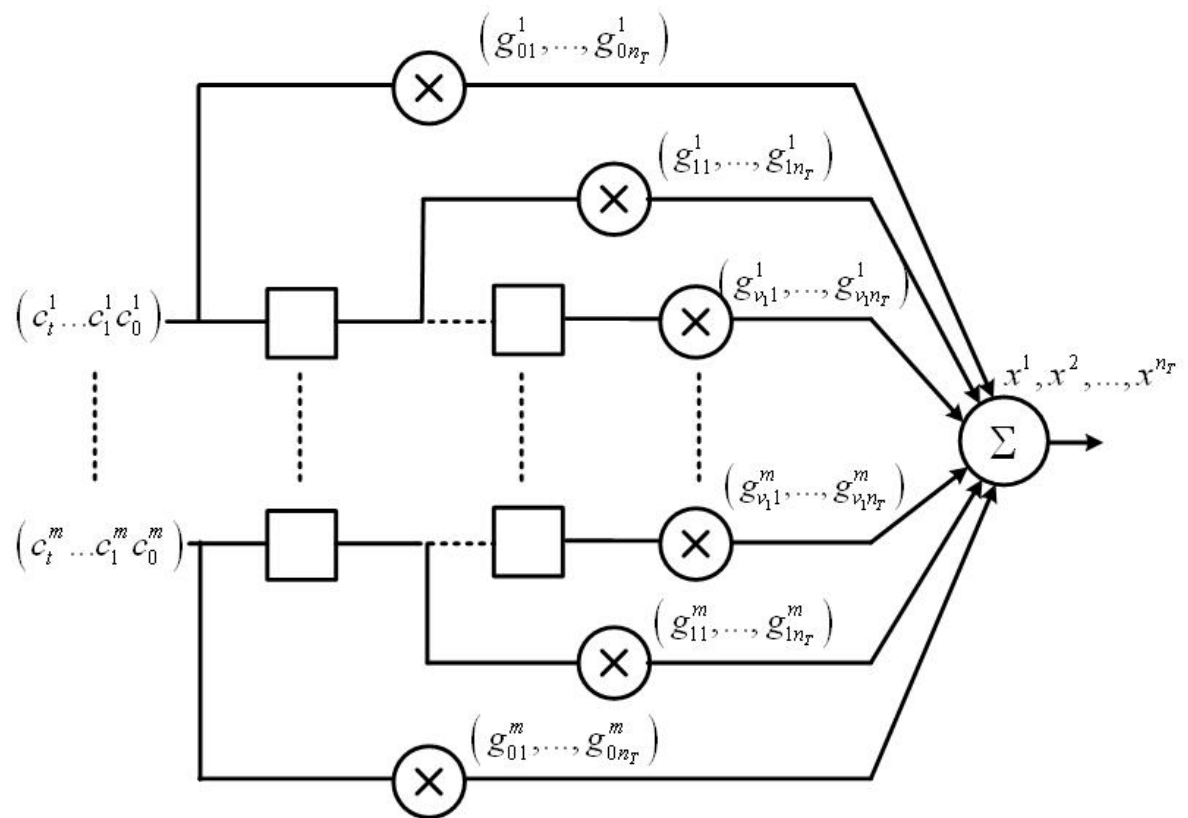


Figure 2.1 Encoder of STTC [12]

For M-PSK modulation, the input sequence of STTC, denoted by \mathbf{c} , is expressed as $\mathbf{c} = (\mathbf{c}_0, \mathbf{c}_1, \dots, \mathbf{c}_t, \dots)$. \mathbf{c}_t , which consists of $m = \log_2 M$ bits, is the input sequence at time t and is given by $\mathbf{c}_t = (c_t^1, c_t^2, \dots, c_t^m)$.

The encoded M-PSK sequence \mathbf{x} , is expressed by $\mathbf{x} = (\mathbf{x}_0, \mathbf{x}_1, \dots, \mathbf{x}_t, \dots)$, where \mathbf{x}_t is a

transmitted symbol at time t and expressed by $\mathbf{x}_t = (x_t^1, x_t^2, \dots, x_t^{n_T})^T$. For a system with n_T transmit antennas, the symbol transmitted through the n -th transmit antenna at time t is denoted by x_t^n .

The m generator coefficient sets is given by

$$\begin{aligned} \mathbf{g}^1 &= \left[\left(g_{0,1}^1, g_{0,2}^1, \dots, g_{0,n_T}^1 \right), \left(g_{1,1}^1, g_{1,2}^1, \dots, g_{1,n_T}^1 \right), \dots, \left(g_{v_1-1,1}^1, g_{v_1-1,2}^1, \dots, g_{v_1-1,n_T}^1 \right) \right] \\ \mathbf{g}^2 &= \left[\left(g_{0,1}^2, g_{0,2}^2, \dots, g_{0,n_T}^2 \right), \left(g_{1,1}^2, g_{1,2}^2, \dots, g_{1,n_T}^2 \right), \dots, \left(g_{v_2-1,1}^2, g_{v_2-1,2}^2, \dots, g_{v_2-1,n_T}^2 \right) \right] \\ &\vdots \\ \mathbf{g}^m &= \left[\left(g_{0,1}^m, g_{0,2}^m, \dots, g_{0,n_T}^m \right), \left(g_{1,1}^m, g_{1,2}^m, \dots, g_{1,n_T}^m \right), \dots, \left(g_{v_m-1,1}^m, g_{v_m-1,2}^m, \dots, g_{v_m-1,n_T}^m \right) \right] \end{aligned} \quad (2.1)$$

where $g_{j,i}^k$, $k = 1, 2, \dots, m$, $j = 1, 2, \dots, v_k$, $i = 1, 2, \dots, n_T$, is an element of the generator coefficient set, and v_k is the memory order of the k -th path. Then we can compute x_t^n as

$$x_t^i = \sum_{k=1}^m \sum_{j=0}^{v_k-1} g_{j,i}^k c_{t-j}^k \bmod M \quad (2.2)$$

The trellis diagram and the performance analysis are studied in [2]. Some STTC such as Tarokh/Seshadri/Calderbank (TSC) codes and Baro/Bausch/Hansmann (BBH) codes are listed in [12].

2.2 STTC with MLSE

In this section, we combine the STTC introduced in the previous section with MLSE on the ISI channel. We propose two schemes to handle ISI. In the first scheme MLSE equalizer is apart from the trellis decoder, which is called ‘‘separated scheme’’. MLSE is used to detect symbols suffering from ISI, and the detected symbols are inputted into the STTC decoder. In the second scheme, the STTC is defined on the complex field, thus the STTC encoder and the ISI channel may be regard as a ‘‘combined channel’’. And we can combine MLSE with STTC decoder in the receiver to handle the ‘‘combined channel’’, and

we call this scheme “combined scheme”. We assume that there are two transmit antennas and one receive antenna.

2.2.1 The separated scheme of STTC with MLSE

The first scheme of STTC with MLSE is illustrated in figure 2.2.

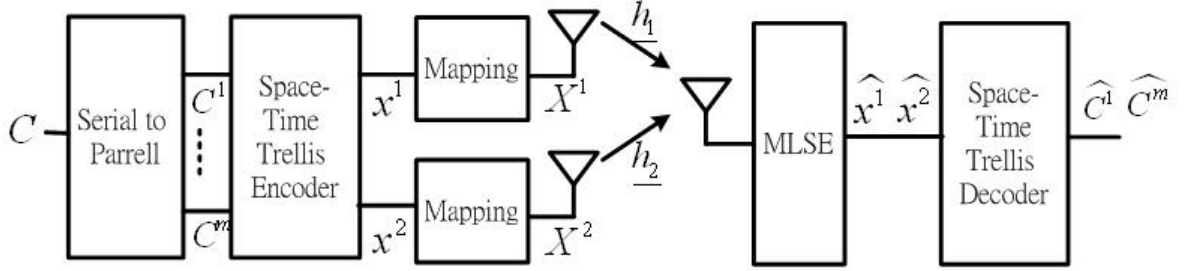


Figure 2.2 The separated scheme

The codeword sequences x^1 and x^2 are expressed in (2.2). After mapping the symbol sequences denoted by $X^1 = [X_1^1, X_2^1, \dots, X_t^1, \dots]$ and $X^2 = [X_1^2, X_2^2, \dots, X_t^2, \dots]$ are transmitted to the ISI channel. Assuming QPSK modulation is used, thus there are two input sequence C^1 and C^2 . According to (2.1) and (2.2), the transmitted symbols are:

$$\begin{aligned}
 x_t^1 &= \sum_{k=1}^2 \sum_{j=0}^{v_k-1} g_{j,1}^k c_{t-j}^k \text{ mod } 4 \\
 &= \left(g_{0,1}^1 C_t^1 + g_{1,1}^1 C_{t-1}^1 + \dots + g_{v-1,1}^1 C_{t-(v-1)}^1 + g_{0,1}^2 C_t^2 + g_{1,1}^2 C_{t-1}^2 + \dots + g_{v-1,1}^2 C_{t-(v-1)}^2 \right) \text{ mod } 4 \\
 x_t^2 &= \sum_{k=1}^2 \sum_{j=0}^{v_k-1} g_{j,2}^k c_{t-j}^k \text{ mod } 4 \\
 &= \left(g_{0,2}^1 C_t^1 + g_{1,2}^1 C_{t-1}^1 + \dots + g_{v-1,2}^1 C_{t-(v-1)}^1 + g_{0,2}^2 C_t^2 + g_{1,2}^2 C_{t-1}^2 + \dots + g_{v-1,2}^2 C_{t-(v-1)}^2 \right) \text{ mod } 4 \quad (2.3)
 \end{aligned}$$

Because QPSK modulation is used, $M=4$ and $m=\log_2 M=2$. And we assume the memory order is the same (i.e. $v_1=v_2=v$) in (2.2) and (2.3).

Then the received signal can be expressed as

$$r = \underline{h}_1 \otimes X_1 + \underline{h}_2 \otimes X_2 + n \quad (2.4)$$

where \underline{h}_1 and \underline{h}_2 are ISI channel presented in (2.4) and n is the noise.

Then the received signals are entered MLSE to solve ISI effect. And the output symbols of MLSE, denoted by x^1 and x^2 , are exploited to decode.

2.2.2 The combined Scheme of STTC with MLSE

STTC encoder and the ISI channel may be regarded as systems with memory. It means the outputs of STTC encoder and the ISI channel both depend on the past and current inputs. Due to the similar property of STTC and the ISI channel, we can combine STTC encoder with ISI channel. The combination of STTC and ISI channel becomes an equivalent channel. Thus in the receiver, MLSE can be also combined with STTC decoder to become another MLSE equalizer which can decode and handle ISI.

However, the STTC in figure 2.2 is defined on the finite field and the ISI channel is defined on the complex field. Thus we can not combine STTC with ISI channel directly. In order to solve this problem, we design a new STTC defined on the complex field, just as the modulated code [13]. The scheme is expressed in figure 2.3.

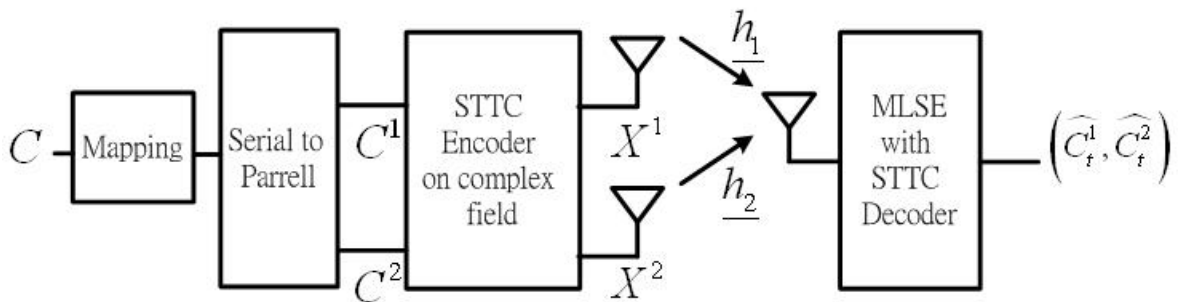


Figure 2.3 The combined scheme

The input sequence C has to be mapped into the complex field first because STTC encoder is defined on the complex field. And we combine STTC encoder with codeword mapping in the transmitter. Then we will derive the equivalent combined channel as follows.

Substituting (2.3) into (2.4) we get

$$\begin{aligned}
r &= \underline{h}_1 \otimes X_t^1 + \underline{h}_2 \otimes X_t^2 + n \\
&= \underline{h}_1 \otimes \left(\sum_{k=1}^m \sum_{j=0}^v g_{j,1}^k c_{t-j}^k \right) + \underline{h}_2 \otimes \left(\sum_{k=1}^m \sum_{j=0}^v g_{j,2}^k c_{t-j}^k \right) + n \\
&= \sum_{k=1}^m \underline{h}_1 \otimes \left(\sum_{j=0}^v g_{j,1}^k c_{t-j}^k \right) + \sum_{k=1}^m \underline{h}_2 \otimes \left(\sum_{j=0}^v g_{j,2}^k c_{t-j}^k \right) + n \\
&= \sum_{k=1}^m \underline{h}_1 \otimes (G_1^k \otimes c_t^k) + \sum_{k=1}^m \underline{h}_2 \otimes (G_2^k \otimes c_t^k) + n \\
&= \sum_{k=1}^m (\underline{h}_1 \otimes G_1^k + \underline{h}_2 \otimes G_2^k) \otimes c_t^k + n \\
&= \sum_{k=1}^m \underline{h}_k' \otimes c_t^k + n
\end{aligned} \tag{2.5}$$

where

$$G_j^k = [g_{0j}^k, g_{1j}^k, \dots, g_{vj}^k], \quad j=1,2 \quad k=1,2,\dots,m \tag{2.6}$$

Remember that the generator coefficients $g_{j,m}^k$ and the computation are defined on GF(4) in (2.2); but in (2.5), $g_{j,m}^k$ and the computation are defined on complex field, thus the computation in (2.5) is valid.

According to (2.5), the combined channels \underline{h}_k' is

$$\underline{h}_k' = \underline{h}_1 \otimes G_1^k + \underline{h}_2 \otimes G_2^k \quad k=1,2 \tag{2.7}$$

In order to get the equivalent combined channel, the generator coefficients $g_{j,m}^k$ must be complex number. The generator coefficients of STTC presented in [12], such as Tarokh/Seshadri/Calderbank (TSC) codes and Baro/Bausch/Hansmann (BBH) codes, is no longer valid in this scheme because they are defined on the finite field. And we have to find new generator coefficients.

The straightforward way is to convert the generator coefficients defined on the finite field, into the complex number. But the method will make a mistake when STTC encoder

generates the codeword by these generator coefficients defined on the complex field. Because modulo-M computation applied in the STTC encoder is a linear computation on the finite field, it is no longer linearly on the complex field. Thus direct conversion of the generator coefficients from finite field to complex field is failed to generate codeword on the complex field.

In this thesis we proposed a STTC transmit scheme which combines the STTC encoding and signal mapping for QAM. First we have to choose a modulation. The values of generator coefficient $g_{j,m}^k$ are dependent on the chosen modulation. For M-QAM and $m=\log_2M$, the generator coefficient are $2^0, 2^1, \dots, 2^{(m/2-1)}$ and $2^0j, 2^1j, \dots, 2^{(m/2-1)}j$. And different arrangement of these coefficients makes different symbols X^1 and X^2 . Some examples are as follows.

Example 1:

Code 1.1, code 1.2 and code 1.3 are all complex STTCs for 4-QAM (QPSK) system with two input sequence. Memory order of the system is two, which means there are one register in each encoding path.

$$\text{Code 1.1: } G_1^1 = (g_{01}^1, g_{11}^1) = (1, 0) \quad , \quad G_2^1 = (g_{02}^1, g_{12}^1) = (1, 0)$$

$$G_1^2 = (g_{01}^2, g_{11}^2) = (j, 0) \quad , \quad G_2^2 = (g_{02}^2, g_{12}^2) = (j, 0)$$

$$\text{Code 1.2: } G_1^1 = (1, 0) \quad , \quad G_2^1 = (0, 1) \quad , \quad G_1^2 = (j, 0) \quad , \quad G_2^2 = (j, 0)$$

$$\text{Code 1.3: } G_1^1 = (0, 1) \quad , \quad G_2^1 = (1, 0) \quad , \quad G_1^2 = (j, 0) \quad , \quad G_2^2 = (0, j)$$

And we can also illustrate the trellis diagram of these codes. Take code 1.3 for example, the trellis structures of code 1.3 are shown in figure 2.4.

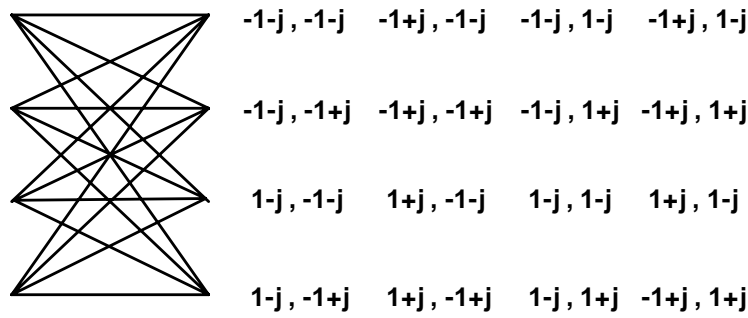


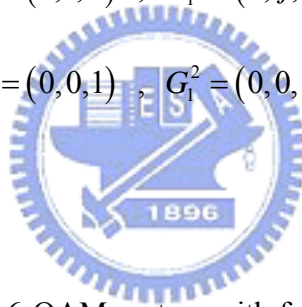
Figure 2.4 Trellis structure for code 1.3

Example 2:

Code 2.1, code 2.2 are complex STTCs for 4-QAM system with two input sequence, and memory order of the system is three.

Code 2.1: $G_1^1 = (1,0,0)$, $G_2^1 = (0,1,0)$, $G_1^2 = (0,j,0)$, $G_2^2 = (j,0,0)$

Code 2.2: $G_1^1 = (1,0,0)$, $G_2^1 = (0,0,1)$, $G_1^2 = (0,0,j)$, $G_2^2 = (j,0,0)$



Example 3:

Code 3 is complex STTC for 16-QAM system with four input sequence, and memory order of the system is two.

Code 3.1: $G_1^1 = (0,2)$, $G_2^1 = (1,0)$, $G_1^2 = (j,0)$, $G_2^2 = (0,j)$,

$$G_1^3 = (0,1)$$
 , $G_2^3 = (2,0)$, $G_1^4 = (2j,0)$, $G_2^4 = (0,2j)$

The coding gains of these codes are almost the same. But we find that systems with different codes achieve different diversity level. Thus we will discuss the code design criterion that achieves the highest diversity level.

The diversity level that the system can achieve is decided by the equivalent combined channel, which is presented in (2.8). If we take QPSK modulation for example, i.e. $m=2$, (2.8) will be written as

$$\begin{aligned}
h_1'(n) &= \sum_{i=0}^{v-1} h_{1,n-i} g_{i,1}^1 + \sum_{i=0}^{v-1} h_{2,n-i} g_{i,2}^1 \\
h_2'(n) &= \sum_{i=0}^{v-1} h_{1,n-i} g_{i,1}^2 + \sum_{i=0}^{v-1} h_{2,n-i} g_{i,2}^2
\end{aligned} \tag{2.9}$$

where $h_i'(n)$ is the n-th element of \underline{h}_i' . The length of $\underline{h}_i'(n)$ denoted by L_i' is $L+v-1$. Thus the diversity level of the system is $L+v-1$ theoretically (When $L+v-1$ is larger than $T_x \times L$, the diversity level will be $T_x \times L$ because it will achieve full diversity.). But if the values of $g_{0,1}^i, g_{1,1}^i, \dots, g_{n-1,1}^i$ and $g_{0,2}^i, g_{1,2}^i, \dots, g_{n-1,2}^i$ are all zero, the first n elements of \underline{h}_i' will also be zero. In this case the diversity level is $L+v-1-n$, thus this STTCs can not achieve the maximum diversity. Similarly, if the values of $g_{v-1,1}^i, g_{v-2,1}^i, \dots, g_{v-n,1}^i$ and $g_{v-1,2}^i, g_{v-2,2}^i, \dots, g_{v-n,2}^i$ are all zero, the last n elements of \underline{h}_i' will be zero. The diversity level that this code can achieve is $L+v-1-n$.

To avoid that the first n or the last n elements are all zeros, the first and the last terms of \underline{h}_i' must not be zero. Thus:

$$\begin{aligned}
h_{11} g_{01}^1 + h_{21} g_{02}^1 \neq 0 \quad , \quad h_{1L} g_{v-1,1}^1 + h_{2L} g_{v-1,2}^1 \neq 0 \\
h_{11} g_{01}^2 + h_{21} g_{02}^2 \neq 0 \quad , \quad h_{1L} g_{v-1,1}^2 + h_{2L} g_{v-1,2}^2 \neq 0
\end{aligned} \tag{2.10}$$

Because $h_{11}, h_{1L}, h_{21}, h_{2L}$ are non-zero complex random variables, we rewrite (2.10) as

$$\begin{aligned}
g_{01}^1 + g_{02}^1 \neq 0 \quad , \quad g_{v-1,1}^1 + g_{v-1,2}^1 \neq 0 \\
g_{01}^2 + g_{02}^2 \neq 0 \quad , \quad g_{v-1,1}^2 + g_{v-1,2}^2 \neq 0
\end{aligned} \tag{2.11}$$

Then consider the simulation result in figure1.8. When the path power distributes averagely, the performance of the system will be better. In general, if the generator coefficient G_1^c and G_1^c are symmetric, where

$$g_{i,1}^c = g_{v-1-i,1}^c \quad , \quad c = 1, 2 \quad , \quad i = 1, 2, \dots, v-1 \tag{2.12}$$

the power of the equivalent combined channel will distribute averagely and will improve the performance. Thus (2.11) and (2.12) are the design criteria of the proposed STTC. We

will verify the criteria by simulation in section 2.2.3.

The complexity of combined scheme is M^{L+v-2} , where M is decided by modulation. Although increasing the memory order often improves the diversity order, the complexity is also increased.

2.2.3 Simulation

The simulation results of the proposed schemes in the previous sections are shown in the section. In our simulation we use the system with two transmit antenna and one receive antenna on the Rayleigh fading channel. The STTC encoder is shown in figure 2.1, and $m=\log_2M=4$ because QPSK modulation is used.

Figure 2.5 shows the simulation of separated scheme and combined scheme on the two-path channel. Based on the same number of registers, the code $G_1^1=(0,2)$, $G_2^1=(2,0)$, $G_1^2=(1,0)$, $G_2^2=(1,0)$ defined on GF(4), is used in separated scheme, and The code $G_1^1=(0,-j)$, $G_2^1=(-j,0)$, $G_1^2=(0,-1)$, $G_2^2=(-1,0)$ defined on the complex field, is used in combined scheme. It is easy to find the better coding gain and diversity gain of combined scheme than separate scheme.

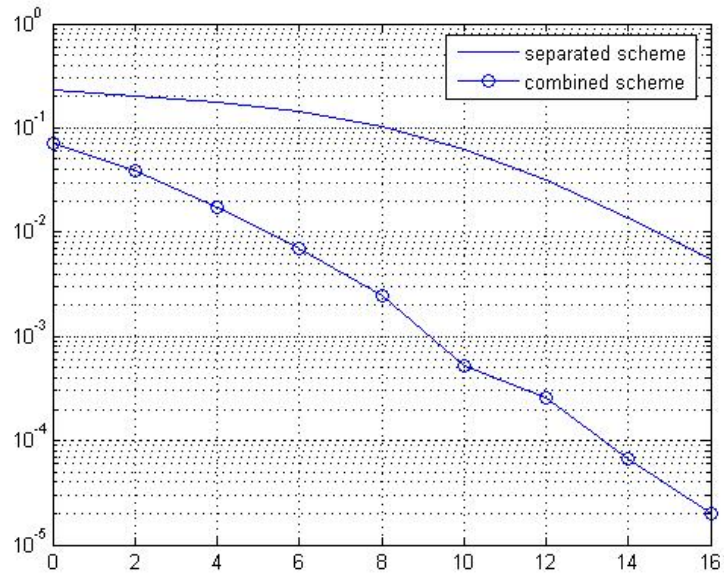


Figure 2.5 Bit error rates of separated scheme and combined scheme

Simulations of code 1.1, 1.2, 1.3, 2.1 and 2.2 in the section 2.2.2 are show in figure 2.6 and figure 2.7. These results are of simulations fits the analysis which mentions in section 2.2.2.

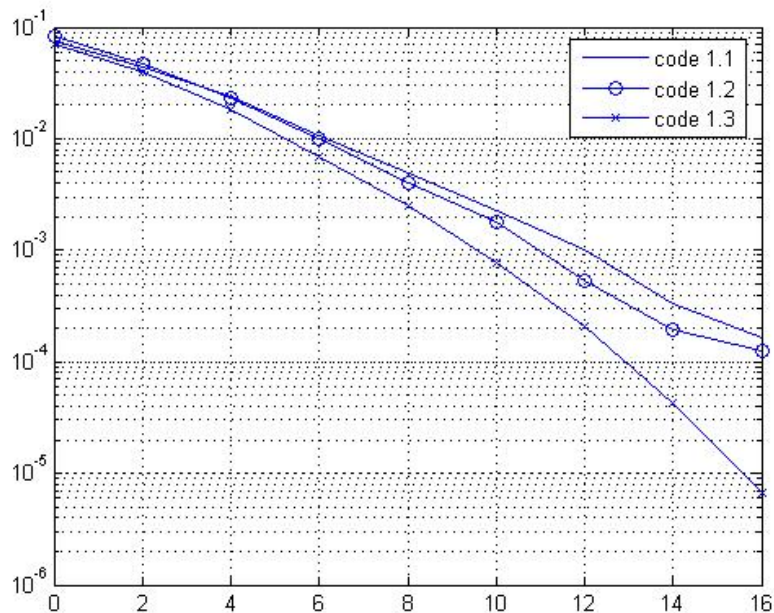


Figure 2.6 Bit error rates of code 1.1 , 1.2 and 1.3

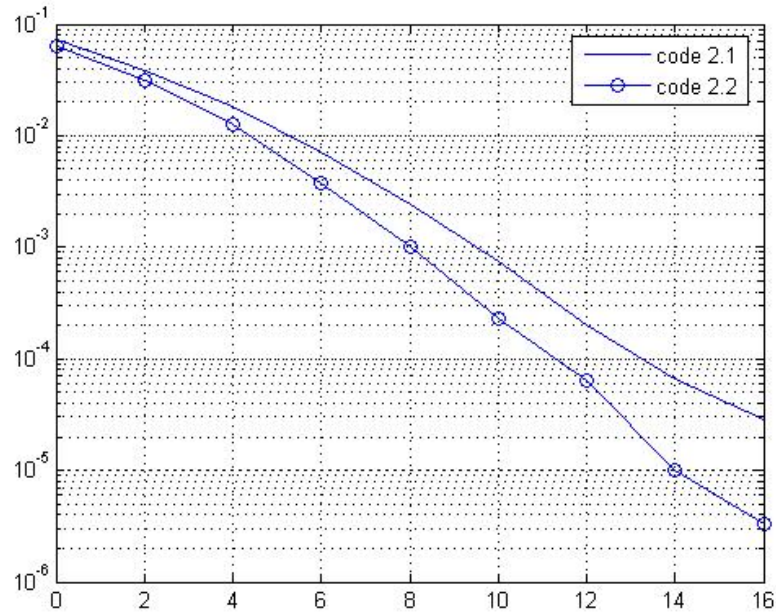


Figure 2.7 Bit error rates of code 2.1 and 2.2

As we describe in section 2.2.2, the maximum diversity order that combined scheme achieves is

$$\text{diversity order} = \begin{cases} L + v - 1 & \text{when } L + v - 1 < T_x L \\ T_x L & \text{otherwise} \end{cases}$$

Figure 2.8 shows the simulation of combined scheme with different memory order on Rayleigh fading channel with two and three paths. The generator coefficients that satisfy (2.11) and (2.12) are chosen for each system. On the two-path channel, the system that memory order is three will achieve full diversity. Therefore increasing the memory order can not improve the diversity order.

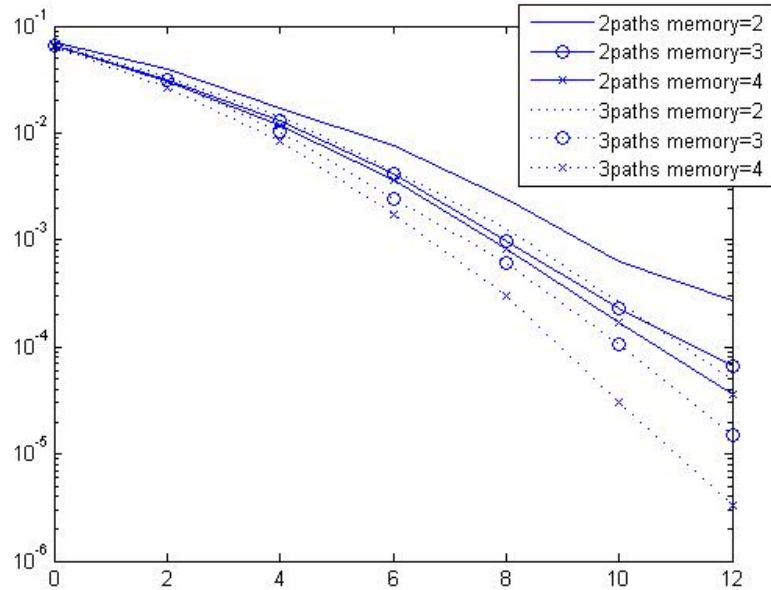


Figure 2.8 Bit error rates of combined scheme

Finally we compare the bit error rates of combined scheme with the other scheme in chapter 1, such as SDD, GDD and Alamouti with MLSE. The results on the channel with two paths and three paths are shown in figure 2.9 and 2.10. Based on the same transmit power and modulation (QPSK), we find remarkable coding gain of combined scheme. Different coding scheme achieve different diversity orders and different complexity.

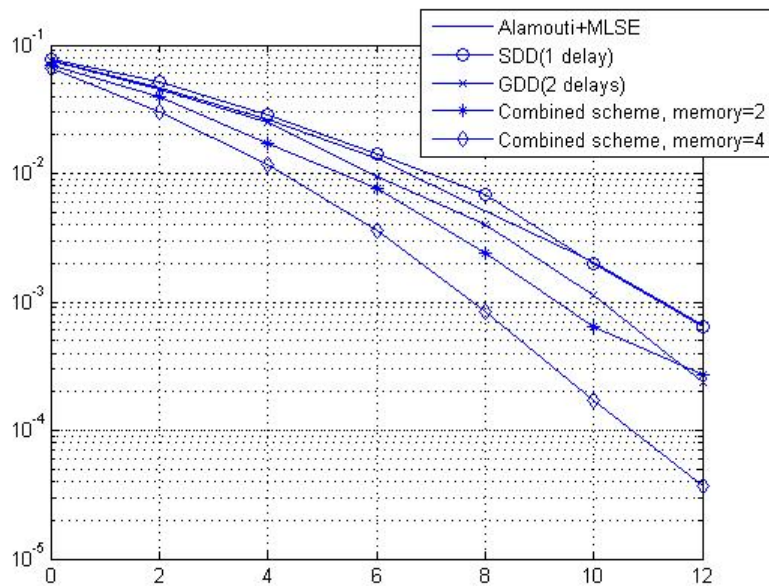


Figure 2.9 Bit error rates of the different schemes on 2-path channel

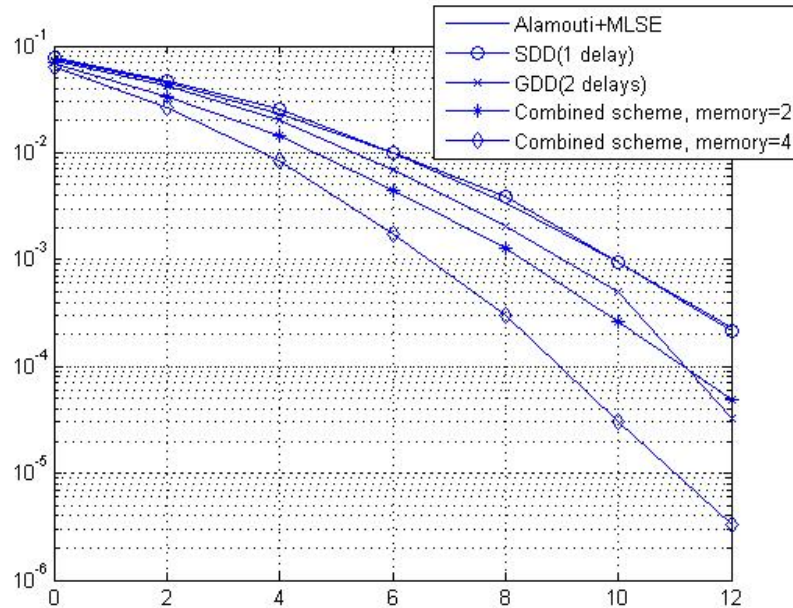


Figure 2.10 Bit error rates of the different schemes on 3-path channel

2.3 Modulated Code

In section 2.2.2, we proposed a new STTC encoder scheme which is defined on the complex field. The basic idea of our proposed STTC is similar to modulated codes, which are error control coding defined on the complex field; therefore modulated codes can be algebraically combined with ISI channel. With modulated codes, ISI is not treated as distortion but diversity and coding gain. The basic conception of modulated codes are introduced in [13] and extended to MIMO system in [14]. We will introduce space-time modulated codes (STMC) and compare it with our proposed STTC in the section.

We assume there are N transmit antennas and M receive antennas. The transmitter scheme of STMC is illustrated in figure 2.11.

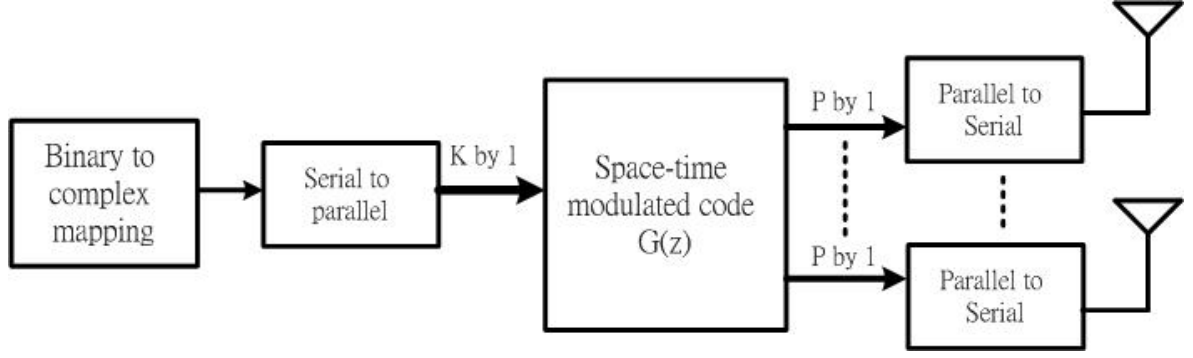


Figure 2.11 Transmit scheme of STMC [15]

The input sequence $C(k)$ is converted to the complex number and then entered $\underline{G}(z)$, which is a rate K/NP STMC encoder. $\underline{G}(z)$ is an NP by K polynomial matrix

$$G(z) = \begin{bmatrix} g_{11}(z) & \dots & g_{1K}(z) \\ \vdots & \vdots & \vdots \\ g_{NP,1}(z) & \dots & g_{NP,K}(z) \end{bmatrix} \quad (2.13)$$

The element of $\underline{G}(z)$, denoted by $g_{ij}(z)$, is the z -transform of encoding coefficients $g_{ij}(n)$.

Thus $g_{ij}(z)$ is expressed as

$$g_{ij}(z) = \sum_n g_{ij}(n) z^{-n} \quad (2.14)$$

And $g_{ij}(k)$ must be under the following condition

$$\sum_{i=1}^{NP} \sum_{j=1}^K \sum_n |g_{ij}(n)|^2 = NP \quad (2.15)$$

The encoded symbols are transmitted on MIMO multipath channel $\underline{H}(k)$. Then we will get the received signal $\underline{R}(k)$. The z -transform of $\underline{R}(k)$ denoted by $\underline{R}(z)$ can be expressed as

$$\underline{R}(z) = \underline{H}(z) \underline{G}(z) \underline{C}(z) + \underline{n}(z) \quad (2.16)$$

where $\underline{C}(z)$ is a K by 1 input sequence and $\underline{n}(z)$ is an NP by 1 white noise vector.

$\underline{H}(z)$, which is the blocked version of $\underline{H}(k)$, can be expressed as

$$\underline{\underline{H}}(z) = \begin{bmatrix} \underline{\underline{H}}_0(z) & z^{-1}\underline{\underline{H}}_{P-1}(z) & \dots & z^{-1}\underline{\underline{H}}_1(z) \\ \underline{\underline{H}}_1(z) & \underline{\underline{H}}_0(z) & \dots & z^{-1}\underline{\underline{H}}_2(z) \\ \vdots & \vdots & \vdots & \vdots \\ \underline{\underline{H}}_{P-2}(z) & \underline{\underline{H}}_{P-3}(z) & \dots & z^{-1}\underline{\underline{H}}_{P-1}(z) \\ \underline{\underline{H}}_{P-1}(z) & \underline{\underline{H}}_{P-2}(z) & \dots & \underline{\underline{H}}_0(z) \end{bmatrix} = \sum_{k=0}^{\Gamma_1} \underline{\underline{H}}_k z^{-k} \quad (2.17)$$

where Γ_1 is the order of $\underline{\underline{H}}(z)$ and $\underline{\underline{H}}_p(z) = \sum_l \underline{\underline{H}}(Pl+p)z^{-l}$, $0 \leq p \leq P-1$.

From (2.16), the combined channel is $\underline{\underline{H}}(z)\underline{\underline{G}}(z)$.

There are several decoding schemes for STMC in [15], such as MMSE (minimum mean square error), joint ZF-DFE (zero-forcing decision feedback equalizer) and MMSE-DFE decoding. In this section, we study the ZF-DFE decoding and corresponding optimal STMC design. We especially focus on the optimization of coding gain. Although different decoding algorithms give different criterion for the optimal STMC design, we can still get the other criterions by similar processing of ZF-DFE.

The STMC ZF-DFE is illustrated in figure 2.12.

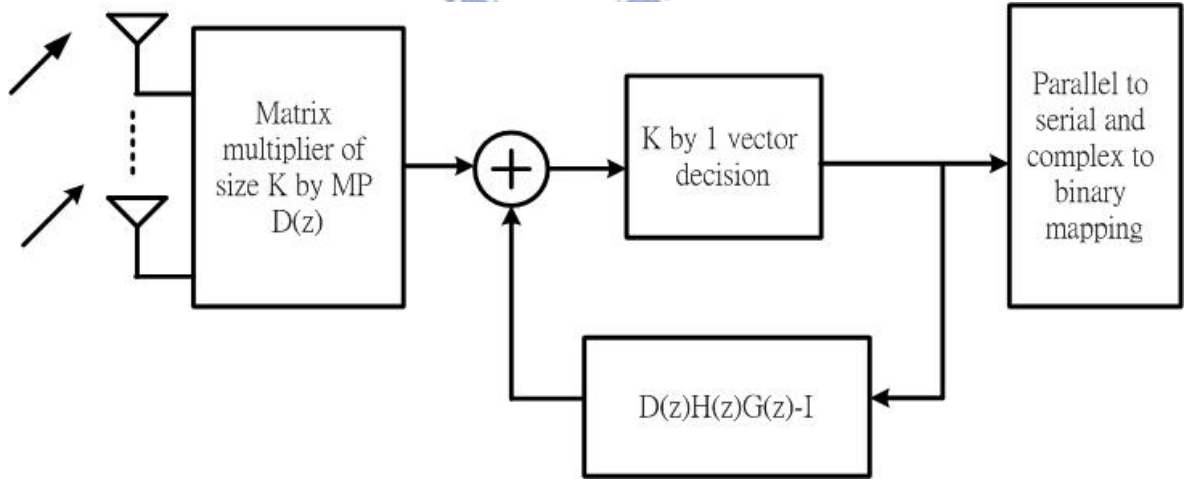


Figure 2.12 STMC ZF-DFE

It is usually the case that the higher the order of the ISI channel to equalize is, the worse the DFE performance is. Thus in [15] it suggests that $\underline{\underline{D}}(z) = \underline{\underline{D}}$ is simply a K by MP constant matrix and STMC encoder takes a block code, i.e., $\underline{\underline{G}}(z) = \underline{\underline{G}}$ is an NP by K

constant matrix.

From the feedback loop in the ZF-DFE, we want to have

$$\underline{\underline{D}}\underline{\underline{H}}_0\underline{\underline{G}} = I_k \quad (2.17)$$

Thus the feedback does not depend on the current vector. After the matrix multiplier the mean power of noise $\tilde{\eta}$ is

$$\sigma_{\tilde{\eta}}^2 = \frac{\sum_{i=1}^K \sum_{j=1}^{MP} |d_{ij}|^2}{K} \sigma_{\eta}^2 = \frac{\sum_{i=1}^K \sum_{j=1}^{MP} |d_{ij}|^2}{2K} N_0 \quad (2.18)$$

And the SNR is

$$SNR = \frac{\sigma_x^2}{\sigma_{\tilde{\eta}}^2} = \frac{2K\sigma_x^2}{\sum_{i=1}^K \sum_{j=1}^{MP} |d_{ij}|^2 N_0} \quad (2.19)$$

In order to maximize the SNR at the receiver in (2.19), the following optimal STMC design rule proposed in [15] is

$$\min_G \sum_{i=1}^K \sum_{j=1}^{MP} |d_{ij}|^2 \quad (2.20)$$

Based on the design rule in (), the bit error rate of STMC on AWGN channel is analysis in [15], and is expressed as

$$BER = Q\left(\sqrt{2 \frac{E_b}{N_0} \frac{\lambda^2 K}{NP}}\right) \quad (2.21)$$

where λ is the singular value of the matrix $\underline{\underline{H}}_0\underline{\underline{G}}$. The minimum of $\sum_{i=1}^K \sum_{j=1}^{MP} |d_{ij}|^2$ in (2.20), is reached if and only if all singular values of $\underline{\underline{H}}_0\underline{\underline{G}}$ are identical.

The optimal STMC $\underline{\underline{G}}_{opt}$ is also derived in [15]

$$\underline{\underline{G}}_{opt} = \underline{\underline{W}}^H \underline{\underline{\hat{G}}} \underline{\underline{U}}_r \quad (2.22)$$

where the singular value decomposition of $\underline{\underline{H}}_0\underline{\underline{G}}$ is $\underline{\underline{U}}_l \underline{\underline{V}} \underline{\underline{U}}_r = \underline{\underline{H}}_0\underline{\underline{G}}$ and the singular

value decomposition of $\underline{\underline{H}}_0^H \underline{\underline{H}}_0$ is $\underline{\underline{W}}^H \underline{\underline{\Lambda}} \underline{\underline{W}} = \underline{\underline{H}}_0^H \underline{\underline{H}}_0$. The matrix $\underline{\underline{\hat{G}}}$ is

$$\hat{\underline{\underline{G}}} = \begin{bmatrix} \text{diag}(\lambda/\xi_1, \dots, \lambda/\xi_K) \\ \underline{\underline{0}}_{(NP-K) \times K} \end{bmatrix} \quad (2.23)$$

where ξ_i is the singular value of the matrix $\underline{\underline{H}}_0^H \underline{\underline{H}}_0$.

Two examples of STMC are presented in [14]. In these two examples, it assumes that $N=M=2$, $K=2$, $P=3$, and two AWGN channel with memory: channel A and channel B.

Channel A is

$$H(0) = H(1) = H(2) = \begin{bmatrix} 0.4762 & 0.4286 \\ -0.3810 & 0.3333 \end{bmatrix}$$

and the optimal STMC for channel A is

$$G_{opt} = \begin{bmatrix} 0.935 & 0.5778 & 0.7498 & 0.4634 & 0.4161 & 0.2572 \\ -0.7529 & 1.2182 & -0.6038 & 0.9769 & -0.3351 & 0.5421 \end{bmatrix}^T$$

Channel B is

$$\begin{aligned} H(0) &= \begin{bmatrix} 0.8111 & 0.5469 \\ 0.7117 & 0.6691 \end{bmatrix}, H(1) = \begin{bmatrix} -0.1459 & -0.0136 \\ -0.0880 & -0.0507 \end{bmatrix} \\ H(2) &= \begin{bmatrix} -0.0183 & -0.1676 \\ -0.1263 & 0.1129 \end{bmatrix}, H(3) = \begin{bmatrix} 0.0154 & -0.0152 \\ -0.0547 & 0.0323 \end{bmatrix} \\ H(4) &= \begin{bmatrix} -0.0620 & -0.0617 \\ -0.0228 & -0.0970 \end{bmatrix} \end{aligned}$$

and the optimal STMC for channel B is

$$G_{opt} = \begin{bmatrix} 0.6276 & 0.4449 & -1.0787 & -0.8155 & 0.5606 & 0.4488 \\ -0.9988 & -0.7658 & -0.0931 & 0.0032 & 0.9498 & 0.7529 \end{bmatrix}^T$$

The simulation results of STMC on channel A and B are shown in figure 2.13.

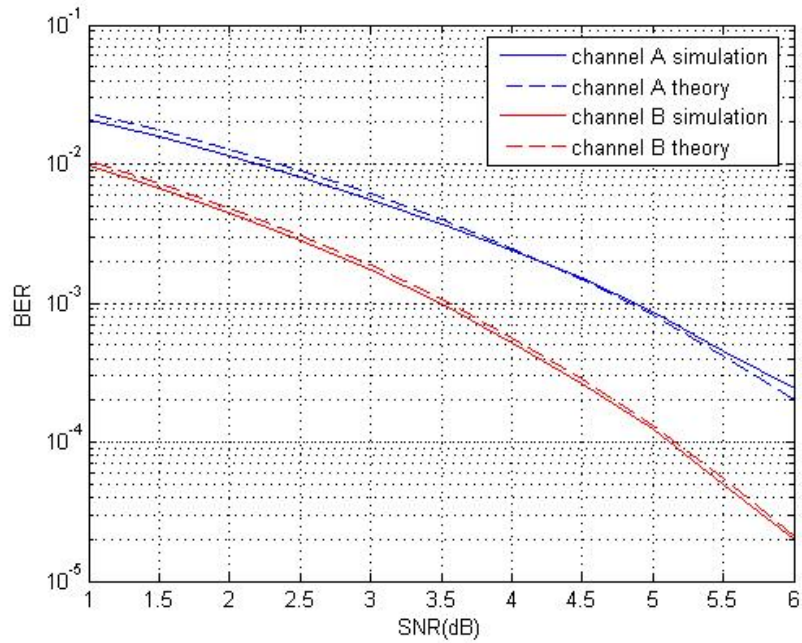


Figure 2.13 Simulations of STMC ZF-DFE on channel A and B

Now we find that the basic idea of modulated codes is similar to our proposed scheme. These two codes are both defined on the complex field to be combined with ISI channel. Thus multipath no longer causes interference, but is exploited to improve the performance of systems. However the purpose is different. We use codes defined on the complex field for joint decoding and achieve multipath diversity gain. But the modulated code is design for exploiting the optimal coding gain from the ISI channel, diversity gain is not emphasized. Because of these reasons there are some difference of transmitter and receiver between modulated codes and our proposed scheme, such as the design of transmitter and receiver.

To achieve the maximum coding gain, the modulated code encoder has to be dependent to the ISI channel. Thus the all the ISI channels for all the different pairs must be known at both the transmitter and the receiver. This condition might be too strong for the wireless channel, especially on the fast fading channel.

The receivers of our scheme and STMC are also different. The STMC ZF-DFE is the decoding scheme which is proposed in [14]. Although it is easier to implement than MLSE,

this scheme can not exploit multipath diversity. Figure 2.14 shows the simulation results of STMC ZF-DFE scheme on the Rayleigh channel with three and five paths. From this simulation we can find that the diversity level is the same no matter the number of paths. Only coding gain is exploited from the channel.

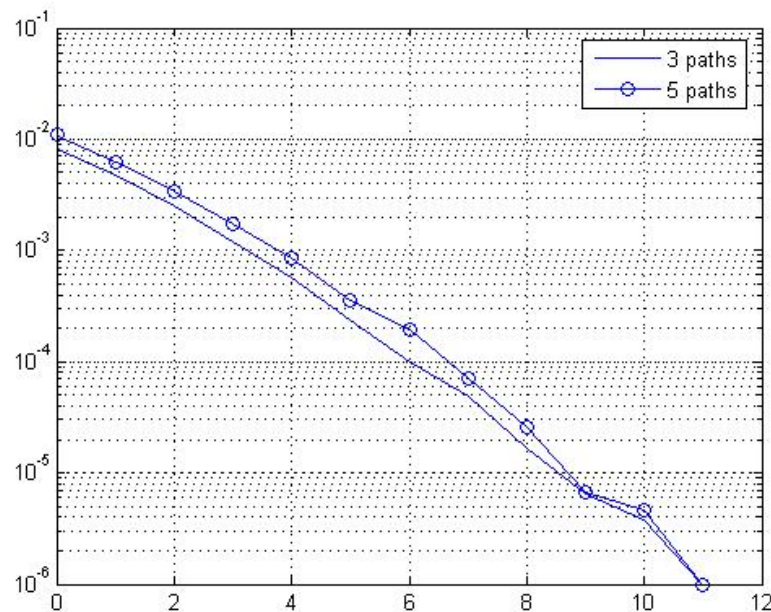


Figure 2.14 Bit error rates of STMC ZF-DFE on Rayleigh fading channel

2.4 Space-Time Turbo Equalization

In the thesis, we analysis the diversity orders that can be achieved by different space-time coding structures. We use MLSE to deal with ISI and exploit the multipath diversity gains because MLSE is an optimal equalization that jointly utilizes the coding, the symbol mapping and the knowledge of channel. However, the computational complexity of this receiver is determined by the channel length and the number of trellis states, which grow exponentially. Because of the high complexity, optimal receiver might be infeasible in most practical system.

In order to approach the remarkable performance of optimal receivers with lower

complexity, turbo equalization [16], an iterative equalization and decoding, is proposed. The transmitter and receiver schemes are illustrated in figure 2.15. The equalizer and the decoder are separated at the receiver. We use BCJR algorithm [17] both in the equalizer and the decoder to estimate the soft information. The soft information from equalizer is interleaved and taken into account in the decoding process. Similarly the soft information from decoder is entered the equalizer, creating a feedback loop between equalizer and decoder. This iterative process will combine the channel information with coding. After iterative process, we expect that the performance of turbo equalizer approach the optimal receiver.

Many reduced complexity turbo equalizers have been proposed. For example, we can use the linear equalizer in place of MAP equalizer. We can also use different codes to improve the performance or reduce the complexity of turbo equalizer. The STTC proposed in section 2.2.2 will be used in turbo equalizer to compare the performance between turbo equalizer and MLSE. And this simulation result is shown in figure 2.16.

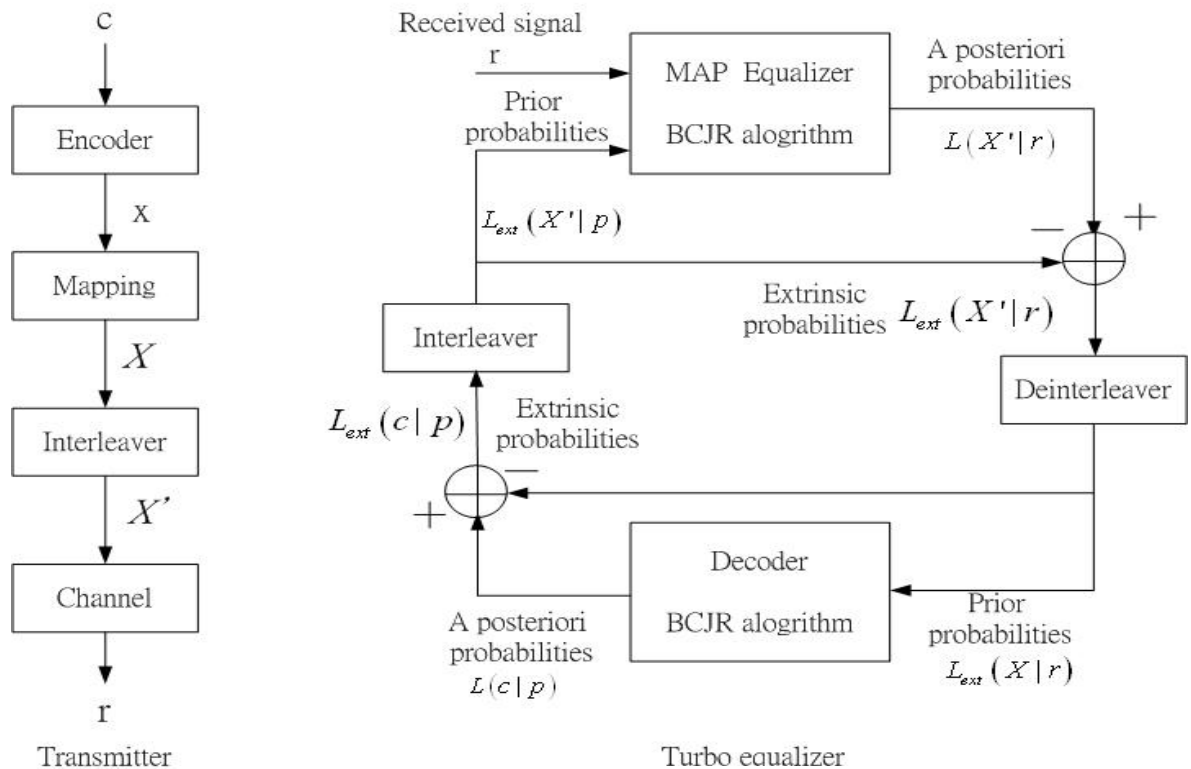


Figure 2.15 The structures of transmitter and turbo equalizer

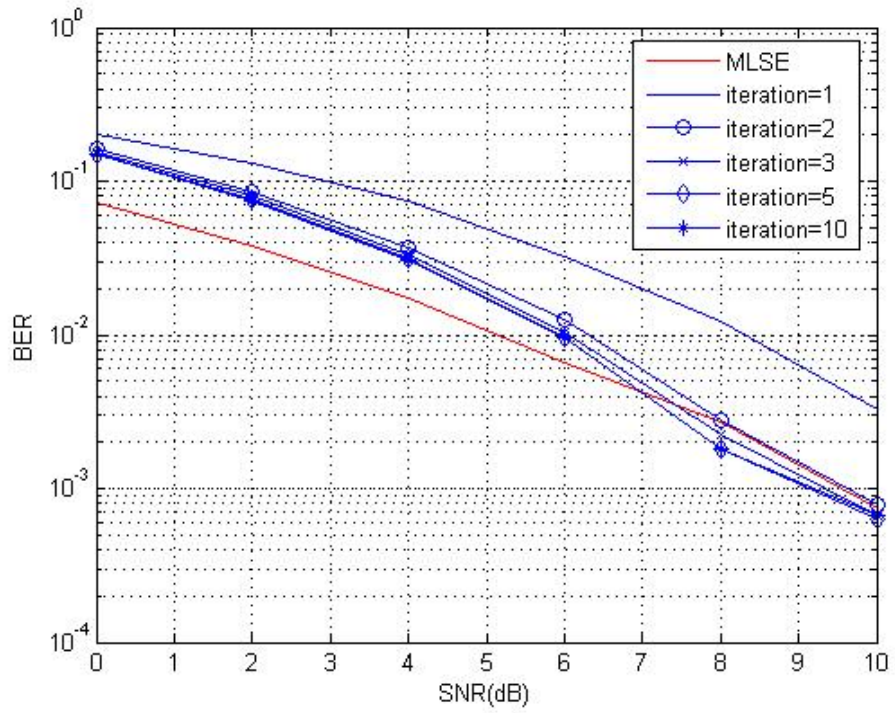


Figure 2.16 Bit error rates of turbo equalizer



Chapter 3

Conclusion

Joint decoding and equalization does provide remarkable benefits in terms of system performance, judging from the simulation results in the thesis. We use MLSE to exploit multipath diversity gain, and analyze the maximum diversity order that can be achieved by different space-time coding schemes. Complexity and application are also discussed in the thesis. Finally we proposed a space-time trellis coding defined on the complex field, thus coding and multipath channel could be combined together. By this complex trellis coding the system could achieve full space and multipath diversity. This coding is also applied in the turbo equalization and other systems.

On the conception of joint decoding and equalization in this thesis, we may extend the coding scheme, which can be combined with channel, to other system with lower complexity than MLSE. Therefore our proposed coding scheme will be more practical.

Reference

- [1] S. M. Alamouti, "A simple transmit diversity technique for wireless communication", *IEEE J. Sel. Areas Comm.*, 16(8), 1451-1458, Oct. 1998.
- [2] V. Tarokh, N. Seshdri and A. R. Calderbank, "Space-Time Codes for High Data Rate Wireless Communication: Performance Analysis and Code Construction", *IEEE Trans. Inform. Theory*, vol.44, no. 2, pp.744-765, Mar. 1998.
- [3] D. Gesbert, H. Bolcskei, D. Gore and A. J. Paulraj, "MIMO wireless channels: capacity and performance prediction", *IEEE Global Telecommun. Conf.* 2000, vol. 2, pp 1083-1088, 2000
- [4] V. Tarokh, N. Seshdri and A. R. Calderbank, "Space-time codes for high data rate wireless communication: Performance analysis and code construction", *IEEE Trans. Inform. Theory*, vol. aa, no. 2, pp. 744-765, Mar. 1998
- [5] E. Lindskog and D. Flore, "Time-reversal space-time block coding and transmit delay diversity- separate and combined", *Proc. Asilomar Conf. on Signals, Systems and Computers*, vol. 1, pp. 572-577, Nov. 2000
- [6] E. Lindskog and D. Flore, "Space-time block coding for channels with intersymbol interference", *Proc. Asilomar Conf. on Signals, Systems and Computers*, 1, 252-256, Pacific Grove, CA, Nov. 2001.
- [7] E. Lindskog and A. Paulraj, "A transmit diversity scheme for channels with intersymbol interference", *Proc. IEEE ICC, 1, 307-311*, New Orleans, LA, 2000
- [8] A. Wittneben, "Base station modulation diversity for digital SIMULCAST", in *Proc. 1991 IEEE Vehicular Technology Conf. (VTC 41st)*, May 1991, pp. 848-853.
- [9] N. Seshadri and J. H. Winters, "Two signaling schemes for improving the error performance of FDD transmission systems using transmitter antenna diversity", in *Proc.*

1993 IEEE Vehicular Technology Conf. (VTC 43rd), May 1993, pp. 508-511.

- [10] J. H. Winters, “The diversity gain of transmit diversity in wireless systems with Rayleigh fading”, in *Proc. 1994 ICC/SUPERC0MM*, New Orleans, LA, May 1994, vol. 2, pp. 1121-1125.
- [11] A. Paulraj, R. Nabar, and D. Gore, “Introduction to Space-Time Wireless Communications”, 1th ed. United Kingdom at the University Press, Cambridge 2003.
- [12] B. Vucetic and J. Yuan, “Space-time coding”, Wiley, Inc, 2003.
- [13] X. G. Xia, P. Fan, and Q. Xie, “A new coding scheme for ISI channel: Modulated codes “, in *Proc. Internal. Conf. Comm.*, Vanconver, Canada, June 6-10 1999
- [14] X. G. Xia, G. Wang, and P. Fan, “Space-time modulated codes for memory channels: Capacity and information rates, zero-forcing decision feedback equalizer“, Technical Report 98-5-2, Department of Electrical and Computer Engineering, University of Delaware, Newark, Delaware, May 1999
- [15] X. G. Xia, “Modulated coding for intersymbol interference channels“, Marcel Dekker, Inc., 2000.
- [16] R. Koetter, A. C. Singer and M. Tüchler, “Turbo equalization”, *IEEE Signal Processing Magazine*, vol. 21, pp. 67-80, Jan. 2004
- [17] S. Lin and J.J. Costello, “Error Control Coding”, Englewood Cliffs, NJ: Prentice-Hall, 1983.